Rainwater chemistry observation in a karst city: variations, influence factors, sources and potential environmental effects

Jie Zeng and Guilin Han

Institute of Earth Sciences, China University of Geosciences (Beijing), Beijing, China

ABSTRACT

The rainwater chemistry and related air contaminants are used to investigate the rainwater ions sources, variations, and influence factors from 2012 to 2014 in Guiyang city (the typical karst urban area of Southwest China). According to temporal rainwater ion concentrations, the obvious variations were presented in the study period, such as Ca^{2+} (125~6,652 μeq L^{-1}) and SO_4^{2-} (11~4,127 μeq L^{-1}). Consequently, Ca^{2+}, Mg^{2+}, SO_4^{2-} and Cl^- are considered as the leading ions. Three critical influencing factors of rainwater ions concentrations, including sources variations, rainfall amount and long-distance migration (rainfall amount > 100 mm) are identified. Based on the typical ionic ratios, source identification suggested that anthropogenic inputs mainly contributed to F^-, NO_3^- and SO_4^{2-}, while the dusts (crustal sources) are the primary sources of Mg^{2+}, Ca^{2+} and K^+. Cl^- Enrichment in long-distance transport is the main contributor of Cl^-. According to the observation of high level of total wet acid deposition, the more detailed spatio-temporal monitoring of rainfall-related acid deposition (particularly sulfur deposition) is required to understand its potential environmental effects in the aquatic ecosystem of the earth surface.

Subjects Atmospheric Chemistry, Ecohydrology, Environmental Contamination and Remediation, Environmental Impacts

Keywords Rainwater chemical, Ionic composition, Source identification, Influence factors, Karst urban area

Submitted 15 December 2020
Accepted 5 March 2021
Published 20 April 2021

Corresponding author
Guilin Han, hanguilin@cugb.edu.cn

Academic editor
Xinfeng Wang

Additional Information and Declarations can be found on page 15

DOI 10.7717/peerj.11167

INTRODUCTION

Wet deposition (rainwater) is a significant sink of atmospheric contaminants, such as sulfur/nitrogen oxides and aerosol (*Benedict et al., 2018*; *Martins et al., 2019*; *Wei et al., 2019*; *Wu et al., 2012*; *Yang et al., 2019*). Two processes including in- and below-cloud procedures are the keys to the elimination of atmospheric pollutants during the entire precipitation process (*Gonçalves et al., 2002*; *Xiao et al., 2013*), and the chemical components and pH are varied concomitantly (*Facchini Cerqueira et al., 2014*; *Larssen et al., 2006*). The chemistry-varied rainwater in different environments can further influence the chemical elemental redistribution and biogeochemical cycles on the earth-surface ecosystem, particularly, aquatic ecosystems (*Bhattarai et al., 2019*; *Martins et al., 2019*). Furthermore, exploring the rainwater chemistry is beneficial for estimating the local atmospheric quality, which could be applied to identify the sources of atmospheric pollutants based on various physical-chemical procedures of different

How to cite this article Zeng J, Han G. 2021. Rainwater chemistry observation in a karst city: variations, influence factors, sources and potential environmental effects. **PeerJ 9:e11167 DOI 10.7717/peerj.11167**

pollutants (*Cereceda-Balic et al., 2020*; *Rouvalis et al., 2009*; *Wei et al., 2020*). The previous work has categorized three types of major ions (chemical species) origins in rainwater, including curst sources (terrestrial dust), marine sources (sea-salt input), and anthropogenic sources (human emission) (*Jain, Madhavan & Ratnam, 2019*; *Liu et al., 2013*; *Xu et al., 2015*). All of the source variations, local meteorology, geomorphology, and environmental protect guidelines affect the rainwater chemical species (*Cable & Deng, 2018*; *Szép et al., 2018*).

A large number of studies in developed regions (e.g., Europe and the United States) have shown that the rainwater chemical components are relatively homogenous on the large temporal-spatial scale due to the common environmental precautions and unified economic development model (*Keresztesi et al., 2019*; *Keresztesi et al., 2020b*; *Mullaugh et al., 2015*). However, the regional economic development is extremely uneven in rapidly developing China (*Wang et al., 2017b*). During the different stages of social-economic development, air contaminants types vary greatly (*Cable & Deng, 2018*; *Cong et al., 2015*), further changing rainwater chemical species in the environmental system (*Jin et al., 2019*; *Xu et al., 2015*). This kind of heterogeneity of rainwater chemistry particularly occurs in the less developed regions of Southwest China (e.g., Guizhou Province), where is the typical continuous distribution area of karst landform over the world (*Liu, Han & Zhang, 2020*). The rainwater-related studies involved in various karst environmental types (urban, forest and agriculture) (*Wu et al., 2012*; *Xiao et al., 2013*). In addition, under the unique geological background of karst landform (such as karst depression and sinkholes), rainfall dominates the migration of surficial material, which makes biogeochemical cycling more sensitive to rainfall event (*Qin et al., 2020*; *Wang et al., 2020*; *Xu et al., 2020*; *Yue et al., 2019*).

In view of the importance of rainfall processes in karst regions, the in-depth investigation of rainwater chemical compositions in the region is necessary, which significantly benefits the better environmental management and improves the knowledge of karst ecological geochemistry. However, the discussions on acid wet deposition (in the form of rainwater) and its potential environmental effect in karst area in related-studies are relatively rare, so there have been few results for comparison across China.

To advance further knowledge of rainwater chemicals in karst urban area, this study took Guiyang, the most typical karst city in SW China, as a case to conduct a systematic investigation based on the 26 monthly mixed rainwater samples collected in May 2012 to June 2014. The aims are to: (1) investigate the rainwater chemical components in the study period, (2) clarify the seasonal variations of rainwater ions and their influencing factors, (3) identify the potential sources of rainwater ions, and (4) explore the possible impacts of rain-associated acid deposition on environment.

MATERIALS & METHODS

Background of study area and sample collection

Guiyang City is the capital of Guizhou Province with a landmass of 8,034 km^2, located in Southwest China (Fig. 1A), which is one of the continuous largest karst regions over world

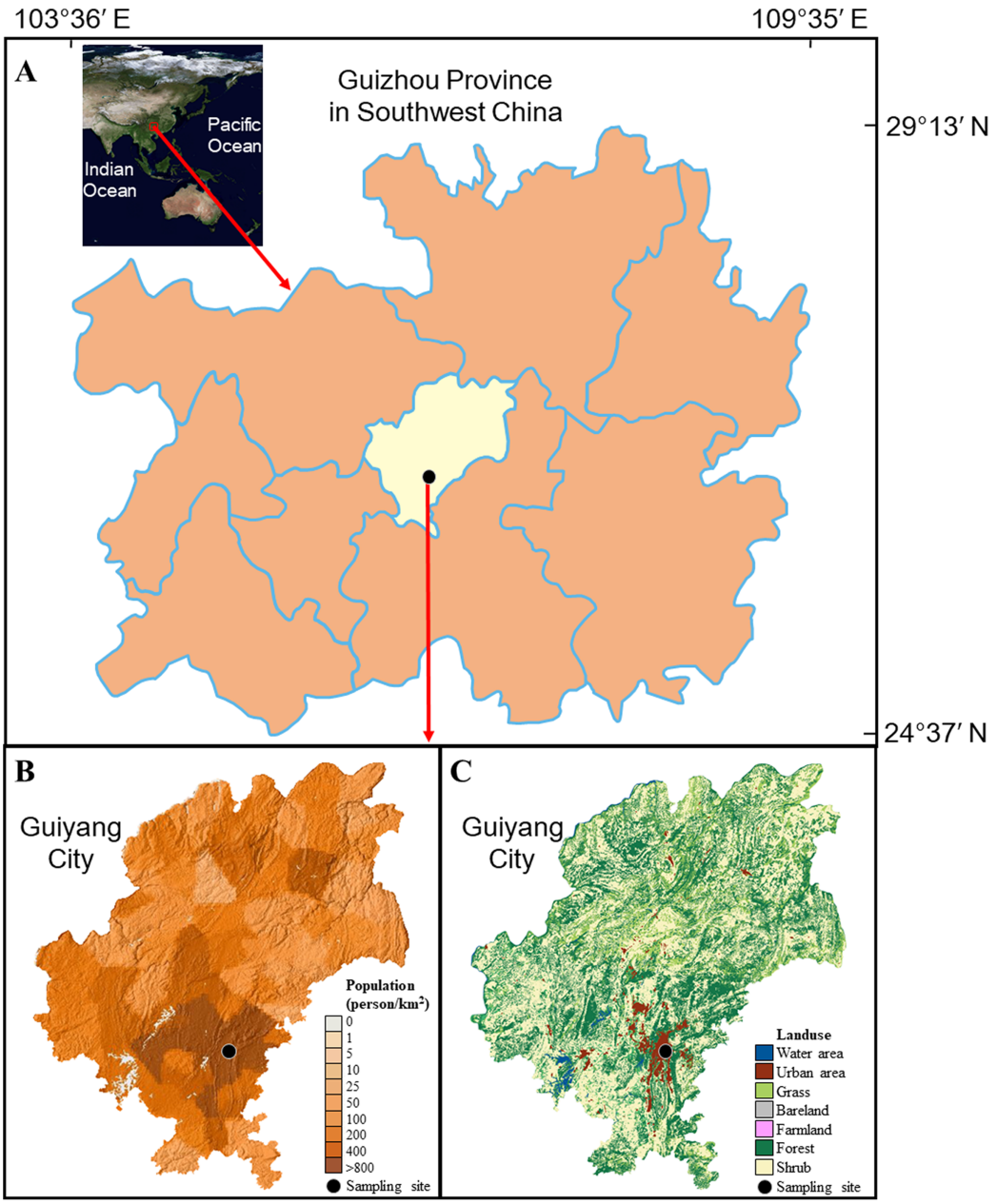

Figure 1 Background of sampling site. (A) the position of Guiyang city; (B) the population density of Guiyang city; (C) the land use of Guiyang city, more details of the surrounding of sampling site can be found in Fig. S1. The data was from Computer Network Information Center of the Chinese Academy of Sciences. Full-size DOI: 10.7717/peerj.11167/fig-1

(*Zeng & Han, 2020*). This city is encircled by hills (elevation ~1,000 m). The karst geomorphology is widespread developed in Guiyang city and carbonate and clastic rocks control the lithology. Subtropical monsoon climate is the characteristic of this city (air temperature ranges from −7.3 to 35.1 °C, with a yearly average of 15.3 °C; average relative humidity is 77%) (*Xiao et al., 2013*). Generally, the seasons can be divided into spring (March to May), summer (June to August), autumn (September to November), and

winter (December to February). Rainfall events mainly happened in wet season (May to October). The annual rainfall amount is 900–1,500 mm.

As a heavily contaminated karst city in southwest China (*Liu et al., 2017*; *Xiao et al., 2013*), more than 4.5 million inhabitants are living here, presenting a high population density (550 people per km^2 in 2013). Most of the population is concentrated in the urban area, making the population density up to 800 people per km^2 and the high degree of urbanization (Figs. 1B and 1C, Fig. S1). The large population results in the emission of atmospheric pollutants, e.g., NO_x derived from high level of traffic (more than 680,000 vehicles in Guiyang city). Since 2003, the air SO_2 concentration in Guiyang has shown a significant decreasing trend, while the air NO_2 concentration increased gradually (Fig. S2A) (*Zhang & Ma, 2016*). The annual mean concentrations of air SO_2 and NO_2 were 0.031 and 0.033 mg m^{-3} in 2013, and 0.024 and 0.031 mg m^{-3} in 2014 (*Yang, Ge & Wu, 2018*; *Zhang & Ma, 2016*). The annual total SO_2 emission and total NO_x emission were about 10.6×10^4 t and 5.7×10^4 t in the study period. The land cover mainly includes water area, urban area, grass land, bare land, farmland, forest, and shrub in the study region (Fig. 1C).

The rainwater samples were collected at the Institute of Geochemistry, CAS, on the central urban built-up area of Guiyang city (26.34 N, 106.43 E, Fig. 1C). This site could well reflect the anthropogenic influence on rainwater in Guiyang city because it is located in the center of the urban built-up area with the highest population density. The polyethylene sampler (set at the place of 15 m over surface) was applied manually to collect rainwater. The polyethylene lid was applied to escape the deposition of atmospheric dust in without-rain days. The sampler was completely cleaned via the deionized-water after each sampling event. The filtration was concluded for each sample by Millipore membrane filters (0.22 μm). The samples after filtration were saved in pre-cleaned polyethylene bottles and kept refrigerated (4 °C). The rainwater samples obtained in each month were proportionally mixed according to the precipitation amount of each precipitation event, and therefore formed a monthly mixed sample. The measured results of mixed sample can denote the monthly weighted-mean values (*Jia & Chen, 2010*). Ultimately, 26 monthly mixed samples were obtained from May 2012 to June 2014. It is noteworthy that the relatively low rainfall amount was observed in 2013 for Guiyang city with almost no rainfall in July (the dotted box in Fig. S2B). That is, the total rainfall amount in 2013 was 888 mm (only ~70% of the previous annual rainfall), which was also far lower than that in 2012 (1,226 mm) and 2014 (1,562 mm). More details about the daily distribution of rainfall amount can be found in Fig. S3.

Measurement of rainwater chemicals

Twenty-six samples were divided into two parts and stored in pre-cleaned polyethylene bottles to measure anion and cation concentrations (HNO_3 acidified, pH < 2). The ion chromatography (IC, DX-120; Dionex Corporation, Sunnyvale, CA, USA) was used to determine the concentrations of major anions, such as NO_3^-, SO_4^{2-}. Cl^-, and F^- with the limit of detection (LOD) of 0.06, 0.10, 0.04 and 0.03 mg L^{-1}. The ICP-AES (IRIS Intrepid-II; Thermo Scientific, Waltham, MA, USA) was applied for detecting the cations

concentrations (Na^+, Ca^{2+}, K^+, and Mg^{2+}) with the LOD of 0.03, 0.04, 0.01 and 0.01 mg L^{-1}.

The procedural blanks, standard reference materials (SRM, GBW08606, National Research Center for Certified Reference Materials, China), and replicates were measured together with all samples to ensure quality control. In brief, the satisfactory repeatability and accuracy for all ions (<5%) were observed in replicate samples and SRM. Moreover, all the measured ions in procedural blank were under the LOD or smaller than 5% of corresponding ions in rainwater samples, implying a trustworthy detected procedure.

Calculation and correlation analysis

To calculate the volume-weighted mean (VWM) concentrations of rainwater ions in the whole study period (May 2012 to June 2014), the equation below is applied (*Zhou et al., 2019*):

$$C = \frac{\sum C_i P_i}{\sum P_i} \tag{1}$$

where C, C_i, and P_i are the VWM concentration of rainwater ions in the whole study period, the ion concentration of each monthly mixed sample, and the monthly rainfall amount, respectively.

For the statistical analyses of rainwater chemical data, the normal distribution of these data is concluded by the Kolmogorov–Smirnov test (K–S test, a non-parametric test usually used to analyze sample data set in environmental research), and Pearson's correlation analyses is therefore applied for potential ion source identification.
The Pearson's correlation coefficient is performed using SPSS 21.0 (IBM, Armonk, NY, USA). Furthermore, the representative air contaminants (PM_{10}, NO_2 and SO_2) are also involved in correlation analysis to clarify the relationship between these species and rainwater ions.

RESULTS

The statistical results of rainwater ion concentrations (monthly ranges and annual VWM values) are summarized and plotted in Fig. 2A. The significant variations in each ion concentration are observed in Guiyang city. That is, all the concentrations of rainwater ions presented a large range, e.g. the Ca^{2+} concentration ranged from 125 to 6,652 μeq L^{-1} and the concentration of SO_4^{2-} fluctuated from 11 to 4,127 μeq L^{-1} (Fig. 2A). Thus, the annual VWM concentrations of each ion are more suitable for comparison. The rainwater ion concentrations in this study followed the sequences based on VWM values: Ca^{2+} (700.1 μeq L^{-1}) > Mg^{2+} (97.0 μeq L^{-1}) > Na^+ (19.6 μeq L^{-1}) > K^+ (14.8 μeq L^{-1}) and SO_4^{2-} (361.4 μeq L^{-1}) > Cl^- (218.3 μeq L^{-1}) > NO_3^- (35.9 μeq L^{-1}) > F^- (20.4 μeq L^{-1}) (Fig. 2A).

Figures 2B and C presented the percentages of each ion, which indicates that SO_4^{2-}, Cl^-, Ca^{2+} and Mg^{2+} are the dominant chemical compositions of rainwater in Guiyang city. SO_4^{2-} and Cl^- account for 56.8% and 34.3% of total measured anions, which are the most and second richest anion (Fig. 2B). The SO_4^{2-} showed the highest percentage, suggesting

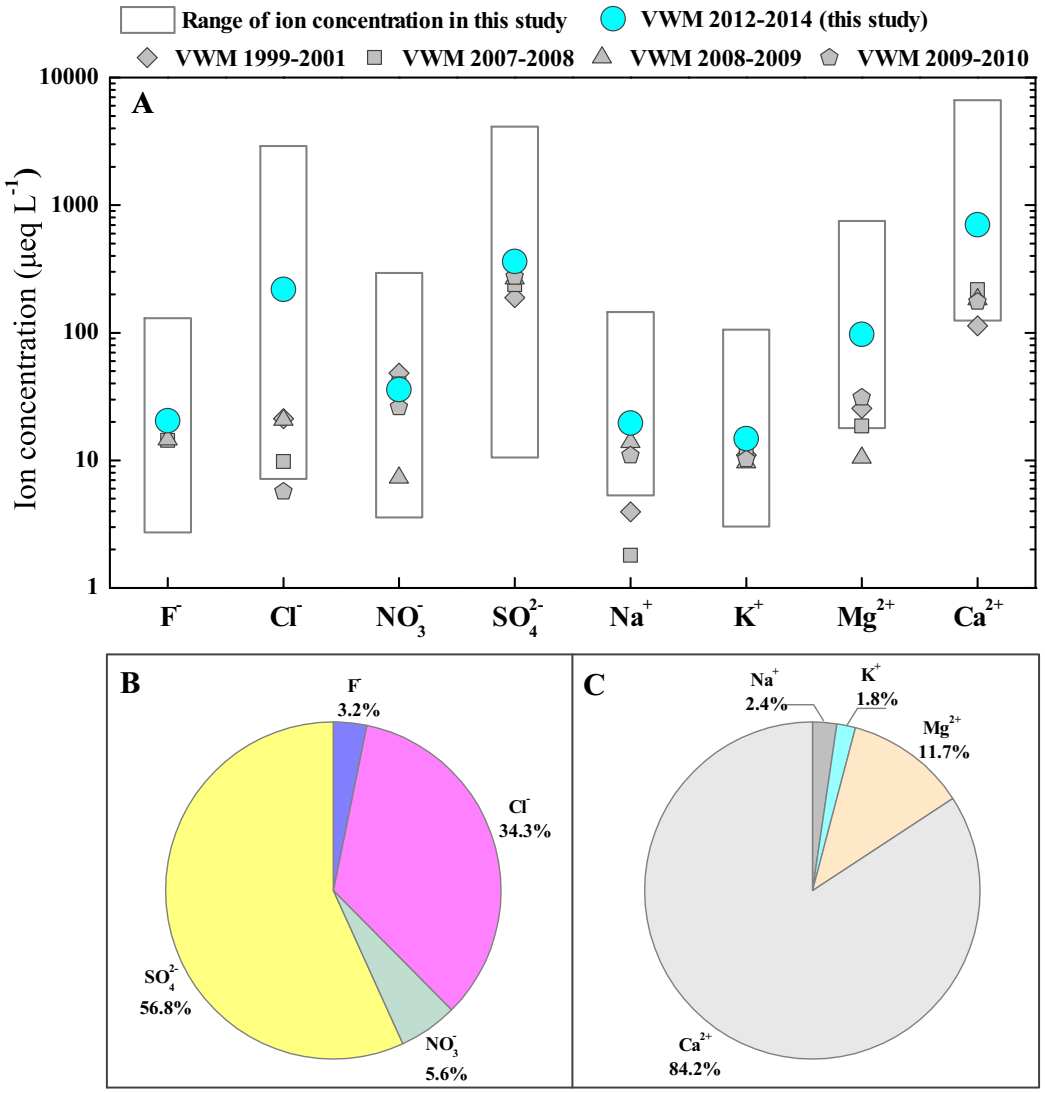

Figure 2 Ion compositions of rainwater in Guiyang city. (A) Overview of rainwater ion contents (μeq L^{-1}) of in Guiyang city, data from previous studies was also included (*Han & Liu, 2006*; *Han et al., 2019*; *Han, Wu & Tang, 2011*; *Xiao et al., 2013*); (B) Rainwater anion composition percentages; (C) Rainwater cation composition percentages. Full-size DOI: 10.7717/peerj.11167/fig-2

the potential effect of strong anthropogenic activities (*Keresztesi et al., 2019*; *Zhou et al., 2019*). In Fig. 2C, Ca^{2+}, Mg^{2+}, Na^{+} and K^{+} account for 84.2%, 11.7%, 2.4% and 1.8% of the total detected cations. Thus, Ca^{2+} is the absolute leading cation and Mg^{2+} is also a more important contributor to cations relative to Na^{+} and K^{+}. Both geology and urbanization are responsible for the cation compositions. The wide-distributed carbonate in karst region is an important potential source of Ca-enriched dust, which can be washed down by rainfall and further be the significant source of rainwater Ca^{2+} (*Han et al., 2019*). Additionally, vast Ca-contained pollutants were continually discharge into the atmosphere due the accelerated development of urbanization (construction industry and other human activities). The aqueous calcium hydroxide was generally applied to remove

Table 1 Comparison of ions concentration (in μeq L^{-1}) of rainwater at Guiyang city and other published data.

Site	F^-	Cl^-	NO_3^-	SO_4^{2-}	Na^+	K^+	Mg^{2+}	Ca^{2+}	Rainwater type
Guiyang (this study)	20.4	218.3	35.9	361.4	19.6	14.8	97.0	700.1	Karst city
Guiyang 1999–2001	—	21.2	48.2	188.0	4.0	11.0	25.5	113.2	Karst city
Guiyang 2007	14.3	9.8	39.6	237.8	1.8	11.1	18.6	217.6	Karst city
Guiyang 2008	14.5	20.7	7.3	265.6	13.9	9.6	10.5	182.9	Karst city
Guiyang 2009	19.9	5.7	26.1	274.6	10.9	10.2	62.2	349.4	Karst city
Puding	2.1	7.3	29.6	130.1	18.8	6.1	16.3	119.6	Karst agriculture
Maolan	0.9	5.1	3.0	40.4	2.4	3.5	3.0	20.8	Karst forest
Prague	2.7	18.3	72.9	129.0	8.0	23.4	10.3	319.9	Bohemian karst
Beijing	12.0	50.9	42.6	357.0	21.5	9.2	53.3	273.0	Inland megacity
Shenzhen	—	45.9	23.7	59.3	36.4	2.0	11.8	18.1	Coastal megacity
Alxa	—	202.8	69.7	471.4	232.5	34.1	72.1	663.0	Desert
Eastern Tien Shan	—	16.5	9.6	53.0	19.0	4.0	18.1	174.2	Mountain area
Yongxing island	—	214.4	8.9	38.0	209.7	5.8	45.6	128.8	Oceanic island

Note:
"—" denotes no data; data sources: Guiyang 1999–2001(*Han & Liu, 2006*), Guiyang 2007 (*Han, Wu & Tang, 2011*), Guiyang 2008 (*Xiao et al., 2013*), Guiyang 2009 (*Han et al., 2019*), Puding (*Zeng et al., 2020*), Maolan (*Zeng et al., 2020*), Prague (*Špičková et al., 2008*), Beijing (*Xu et al., 2015*), Shenzhen (*Zhou et al., 2019*), Alxa (*Rao et al., 2017*), Eastern Tien Shan (*Zhao et al., 2008*), Yongxing island (*Xiao et al., 2016*).

the sulfur dioxide emitted from coal-fired industries (wet desulfurization) (*Garea et al., 1996*; *Wang et al., 2017a*), which is another potential source of atmospheric Ca, in particular, since the effective implementation of environmental protection policies, such as National Acid Rain and SO_2 Pollution Prevention Plan (*Wen et al., 2020*; *Yu et al., 2019*). In summary, Ca^{2+} and Mg^{2+} concentrations make up 95.9% of cations, and SO_4^{2-} and Cl^- make up 91.1% of anions.

DISCUSSION

Comparison between different zones

We listed the rainwater ion concentration in Guiyang city, together with historical data in Guiyang city, and those published data in various eco-environmental systems (Table 1). In historical comparison, all ion concentrations in the study period (May 2012 to June 2014)were higher than those historical data, with the exception of NO_3^- that slightly lower than 2007 (Fig. 2A and Table 1) (*Han & Liu, 2006*; *Han et al., 2019*; *Han, Wu & Tang, 2011*; *Xiao et al., 2013*). In particular, the Cl^- concentration of this study showed a level comparable to that of oceanic rainwater (Table 1) (*Xiao et al., 2016*), which reflects that the Cl^- was underwent the very strong process of enrichment and concentration (indicates potential anthropogenic input) during the transportation of atmospheric clouds (*Jain, Madhavan & Ratnam, 2019*), while the HCl-released reaction caused Cl^- depletion was negligible. Overall, rainwater ion concentrations in Guiyang city were on the rise. For the horizontal comparison, the concentrations of most ions (Cl^-, F^-, SO_4^{2-}, Na^+, Ca^{2+} and Mg^{2+}) of rainwater in this study is higher than that in other karst areas (Table 1), including karst agricultural area (Puding), karst forest area (Maolan), Bohemian karst area

(Prague) (*Špičková et al., 2008*; *Zeng et al., 2020*). Only the K^+ and NO_3^- concentrations of rainwater in Guiyang city are lower than those of rainwater in Bohemian karst area (*Špičková et al., 2008*). This reveals the impact of the different intension of local human emission (e.g., transportation emissions, fossil fuel burning, agricultural production) on rainwater ionic species under various karst environmental types. Moreover, it is noteworthy that the concentrations of SO_4^{2-} and NO_3^- (typical human-derived ions) in Guiyang city are close to that in inland megacity (Beijing) (*Xu et al., 2015*), and the concentrations of Ca^{2+} is even higher than that of desert environment (Alxa) (*Rao et al., 2017*).

Temporal variation, influencing causes and neutralization coefficients of ion compositions

The highest total ion concentrations were found in cooler months (October to March), while the warmer months (April to September) were accompanied by the lowest concentrations (Fig. 3). All ions displayed the parallel temporal change trends, which can be interpreted by two factors. First, the temporal change of potential substance origin is the significant factor of rainwater ions concentrations variation, such as the change of air particulate matter (high content of Ca^{2+}) and gaseous air pollutants (*Jain, Madhavan & Ratnam, 2019*). This can be further supported by the observed monthly variations in air PM_{10}, SO_2, and NO_2 content, that is, the high/low concentrations of rainwater Ca^{2+} was accompanied by high/low air PM_{10}, SO_2 and NO_2 content (Figs. 3A and 3B). These related parameters show significant positive correlation. The correlation coefficients ($p < 0.05$) are 0.58, 0.74 and 0.51 between Ca^{2+} and air PM_{10}, SO_4^{2-} and air SO_2, and NO_3^- and air NO_2, respectively. Second, the relative frequent rainfall event in wet season (warmer months) can effectively wash down the various atmospheric components, and further result in the air contaminants could not have a long retention time compared to dry season (warmer months) (*Xiao & Liu, 2002*), while more air components are scoured by rainwater in dry season with little rainfall (*Szép et al., 2019*).

Overall, the ions concentrations presented a converse temporal trend to the precipitation amount from the monthly scale (Fig. 3). This revealed that precipitation amount is the important factor impacting rainwater ionic species, which is in agreement to the previous findings (*Keresztesi et al., 2020b*; *Szép et al., 2018*). The more clear relationship between rainfall amount and ions concentrations were illuminated in Figs. 4A–4H. The further correlation analysis of ions concentrations and precipitation amount after logarithmic computation (Figs. 4I–4P) revealed that ions concentrations in Guiyang city are observably impacted by the dilution effect (or scouring effect) under large rainfall amount (e.g., $r = -0.84$ for Ca^{2+} and $r = -0.77$ for SO_4^{2-}, $p < 0.05$), which is commonly found in other areas (*Silva, Gonçalves & Freitas, 2009*; *Szép et al., 2018*). In this scouring process, the air components, such as sulfur/nitrogen oxides, Mg and Ca-mineral, and particulate nitrate (e.g., nitrated phenols (*Li et al., 2020b*)) are powerfully scoured down (below-cloud processes) during the early rain-stage, causing the high ionic concentration observed under the low precipitation amount condition (*Jia & Chen, 2010*). In contrast, without the continuous supplements of gaseous air contaminants or suspended matters,

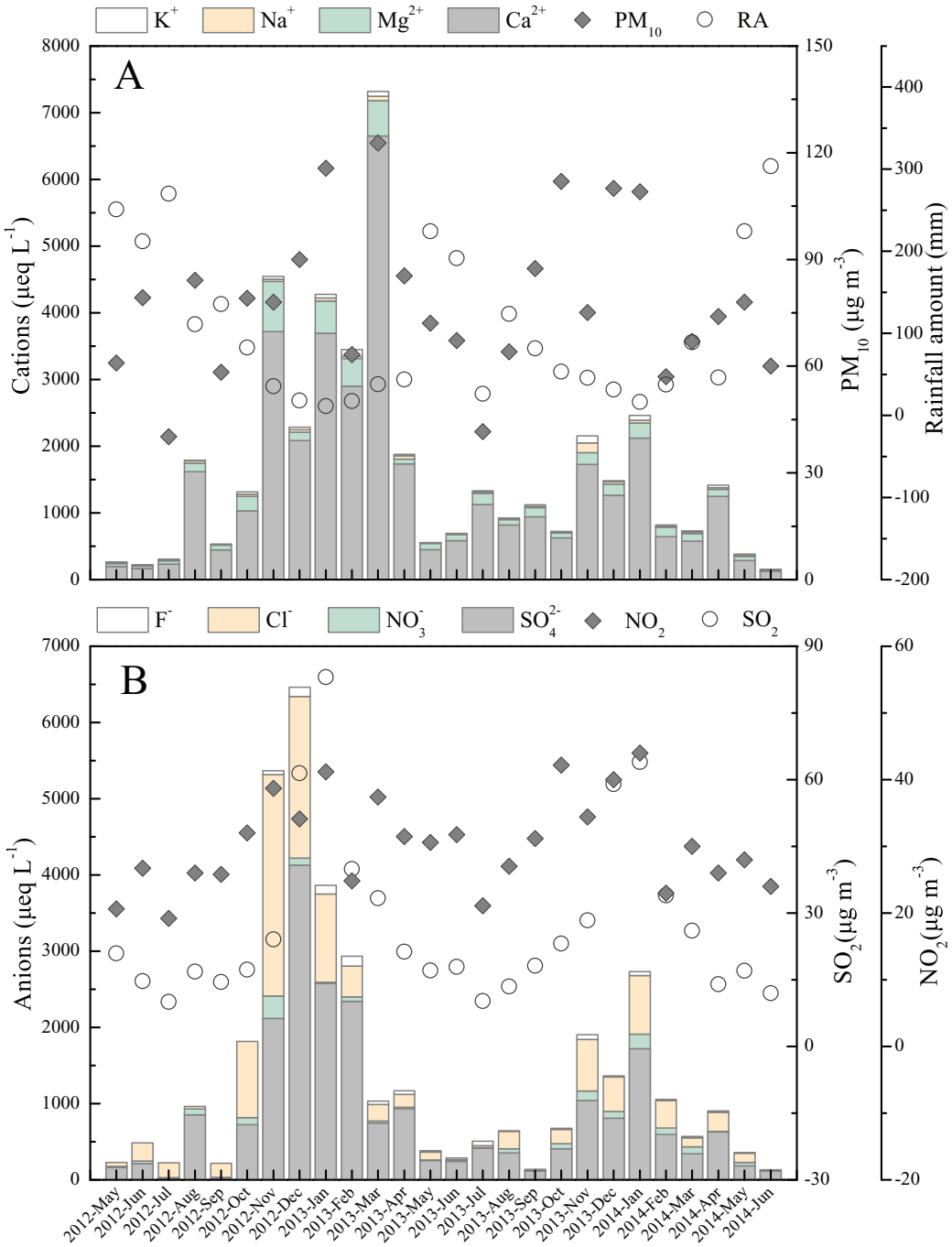

Figure 3 **Monthly variations in ion concentrations and other parameters.** (A) Cations concentration, PM_{10}, rainfall amount (RA); (B) anions concentration and atmospheric SO_2 and NO_2 content. The PM_{10} and air SO_2 and NO_2 data are from literature (*Yang, Ge & Wu, 2018*; *Zhang & Ma, 2016*)
Full-size DOI: 10.7717/peerj.11167/fig-3

the ionic concentration of the late rain-stage (prolonged precipitation event) is decreased progressively and stayed at a low content level (Figs. 4A–4H) (*Gonçalves et al., 2002*). It is noteworthy that the critical point to distinguish between early and late rain-stage is ~100 mm for all ions from Figs. 4A–4H. This indicates that the various species in the

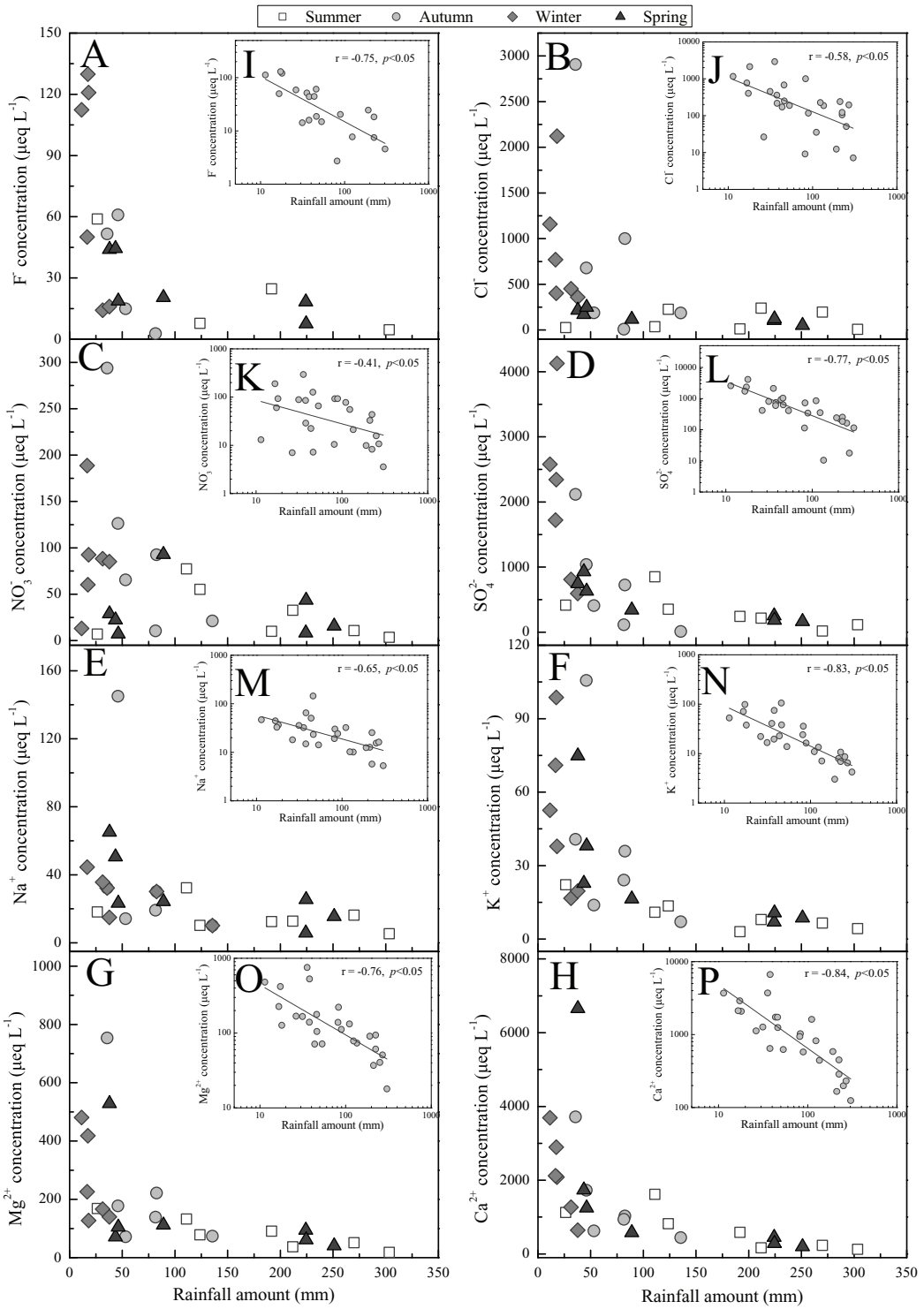

Figure 4 Relationships between ions concentrations and rainfall amount in Guiyang city from 2012-Summer to 2014-Spring. A–H represent the relationships between rainfall amount and F^-, Cl^-, NO_3^-, SO_4^{2-}, Na^+, K^+, Mg^{2+}, and Ca^{2+}; I–P are the corresponding logarithmic ion content vs. logarithmic rainfall amount.

Full-size DOI: 10.7717/peerj.11167/fig-4

atmosphere are almost washed down completely within the precipitation of 100 mm, and the similar critical points (different rainfall values) were observed in previous studies (*Silva, Gonçalves & Freitas, 2009*; *Xiao et al., 2013*; *Zeng et al., 2020*). Conversely, if the precipitation amount exceeds 100 mm, the rainwater ion concentrations decreased insignificantly with the increase of rainfall amount and even stayed at a basically constant and very low concentration level (Figs. 4A–4H). At this time, the rainwater ionic contents primarily reveal in-cloud processes, that is, the ionic concentration of rainwater is similar to the cloud-water (gas/aerosols-dissolved cloud drops) (*Rao et al., 2017*; *Silva, Gonçalves & Freitas, 2009*). Under such condition (precipitation >100 mm), the scouring effect is negligible, while the long-range transportation is regarded as the most critical reason influencing rainwater ionic compositions (*Gonçalves et al., 2002*).

To gain more information regarding to the neutralization coefficients of different alkaline ions in rainwater, the VWM concentrations-based neutralization factors (NFs) were calculated according to the equation: NF of X = $[X]/[NO_3^- + SO_4^{2-}]$, where X= Na^+, K^+, Mg^{2+}, Ca^{2+} (*Xiao et al., 2013*). The NF values of Na^+, K^+, Mg^{2+} and Ca^{2+} in rainwater at Guiyang city were 0.05, 0.04, 0.24 and 1.76, respectively. These results suggest that Ca^{2+} is the dominant neutralization alkaline ion in the rainwater, following by the ions of Mg^{2+}, Na^+, and K^+, which also indicate the significant potential influence of Ca-enriched substances derived from the construction industry and windblown dust. Furthermore, the enrichment factors (EF) of ions in rainwater relative to the corresponding ions in seawater/crust were calculated as: $EF_{seawater}=[X/Na^+]_{rainwater}/[X/Na^+]_{seawater}$; $EF_{crust} =[X/Ca^{2+}]_{rainwater}/[X/Ca^{2+}]_{crust}$, where the ion equivalent ratios of $[X/Na^+]_{seawater}$ and $[X/Ca^{2+}]_{crust}$ were followed the previous work (*Berner & Berner, 1987*; *Rudnick & Gao, 2004*). The $EF_{seawater}$ of K^+, Mg^{2+}, SO_4^{2-} and Ca^{2+} was calculated as 35, 22, 152 and 814, while the EF_{crust} of K^+, Mg^{2+} and Na^+ were 0.05, 0.14 and 0.03. These results significantly suggest that most of the rainwater ions were concentrated relative to the seawater, but depleted relative to the earth's crust.

Source of major ions

Since the alike physico-chemical natures and potential co-sources of some atmospheric components (e.g., SO_x and NO_x) (*Vet et al., 2014*), the correlation coefficient is a frequently-used tool for exploring the common origins of rainwater chemical components (*Xing et al., 2019*), which is applied in this study. As shown in Fig. 5, the significant negative correlations are presented between precipitation amount and all ions and air pollutants ($p < 0.05$), which further confirms the important effect of precipitation amount on the variations in ionic concentrations. However, obvious positive correlations are observed between most of ion components, such as r = 0.85 for Ca^{2+} and Mg^{2+}, r = 0.87 for SO_4^{2-} and F^-, r = 0.77 for SO_4^{2-} and Cl^-, and r = 0.45 for SO_4^{2-} and NO_3^- (Fig. 5), it is thereby difficult to obtain further origin information of rainwater ion by correlation analysis.

To identify further the associations of various ions of rainwater and the potential origins, the representative ionic ratios (in equivalent concentration, e.g., Cl^-/Na^+, SO_4^{2-}/NO_3^- and Mg^{2+}/Ca^{2+}) are presented in Fig. 6A. The low Cl^-/Na^+ ratios (compared with seawater) are only found in few samples, while most samples present a higher Cl^-/Na^+

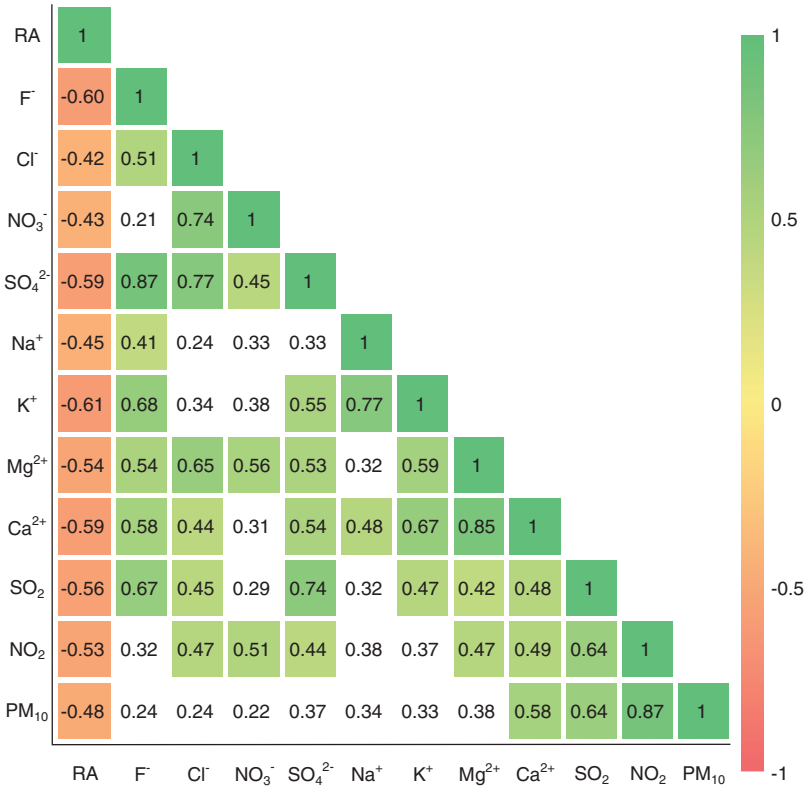

Figure 5 Pearson correlation coefficients between major ions in rainwater and other parameters in Guiyang city. RA, rainfall amount; white cells denote statistically non-significant correlations ($p > 0.05$), while other cells denote the significance level of $p < 0.05$. Full-size DOI: 10.7717/peerj.11167/fig-5

ratio relative to seawater (*Berner & Berner, 1987*). In total, the rainwater Cl^-/Na^+ ratios in this study (karst urban area) are also much greater than that in karst agricultural regions (*Zeng et al., 2020*). In combined with the high Cl^- concentrations (comparable to the Cl^- in marine rainwater) and relative low Na^+ concentrations (Table 1), here we conclude that the sea salt input Cl^- was intensively enriched in the transported processes of atmospheric clouds (*Jain, Madhavan & Ratnam, 2019*; *Xiao et al., 2013*), while the Na^+ may be reduced in some degree due the input of other cations. That is, there are other potential sources of Cl^- besides marine sources. The relationship between Cl^- and the typical anthropogenic inputs SO_4^{2-} (r = 0.77 for SO_4^{2-} and Cl^-) further support this. Previous work has shown that the chlorinated chemical plants emissions and combustion of chlorinated organics in some coal combustion industries are the important anthropogenic sources of rainwater Cl^- (*Facchini Cerqueira et al., 2014*; *Keresztesi et al., 2019*; *Wu et al., 2012*). Moreover, the facilities using large amounts of disinfectants (Cl-contained) is also another potential source of rainwater Cl^-, such as the hospitals near the sampling site (Guizhou Electric Power Workers Hospital, and Guiyang First People's Hospital) and other place (e.g., swimming pool). Thus, here we attributed the high contents of rainwater Cl^- were caused by the potential coal combustion industries, disinfectants-used facilities and the Cl^- enrichment in long-distance transportation. Furthermore, most rainwater samples present high SO_4^{2-}/Na^+ and NO_3^-/Na^+ ratios

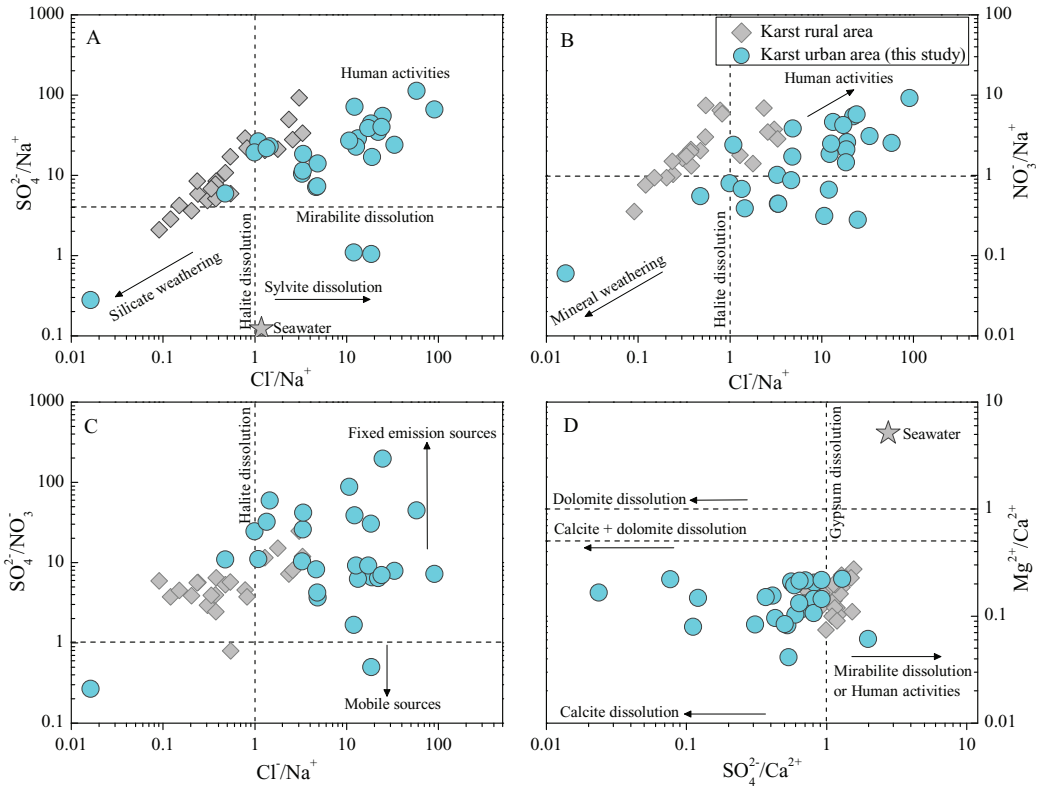

Figure 6 The relationship between the ratios of typical ions (equivalent ratio) in karst urban and rural rainwater. (A) SO_4^{2-}/Na^+ vs. Cl^-/Na^+, (B) NO_3^-/Na^+ vs. Cl^-/Na^+, (C) SO_4^{2-}/NO_3^- vs. Cl^-/Na^+, and (D) Mg^{2+}/Ca^{2+} vs. SO_4^{2-}/Ca^{2+} ratio. Data sources for karst rural rainwater chemistry and other reference values are from (*Berner & Berner, 1987*; *Zeng et al., 2020*).

Full-size DOI: 10.7717/peerj.11167/fig-6

(Figs. 6A and 6B), indicating the significant impact of anthropogenic input (human activities), that is, these anions (SO_4^{2-} and NO_3^-) are mainly derived from anthropogenic emissions (*Keresztesi et al., 2019*; *Xu et al., 2015*). Especially, SO_4^{2-}/NO_3^- ratio exceed 1 is observed in almost all samples, even up to 198 (Fig. 6C), further reflecting the leading role of fixed contamination emission origins, e.g., transportation/diffusion of the coal-burning emissions (*Li et al., 2020a*; *Naimabadi et al., 2018*), whereas the mobile sources contribution (mainly vehicle emissions) and its long-range transport/diffusion are relative muted (*Rao et al., 2017*). In Fig. 6D, all the sample symbols are plotted between the lines of (calcite + dolomite dissolution) and (calcite dissolution) due to the small Mg^{2+}/Ca^{2+} ratios (0.04–0.22), implying the primarily influence of calcite dissolution of atmospheric dust derived from different carbonate weathering processes on Ca^{2+} and Mg^{2+} in rainwater (*Keresztesi et al., 2020a*; *Lü, Han & Wu, 2017*). On the contrary, the sea salt contribution to the rainwater cations is very limited (based on the comparison with seawater cations ratio in Fig. 6D). In addition, although F^- and K^+ related ionic ratios are not shown in Fig. 6, the previous work has indicated that the biomass burning (e.g., straw combustion) and soil dust are the main sources of K^+ and the anthropogenic

emissions can be a interpretation for the higher F^- concentration in rainwater (*Khare et al., 2004*; *Zhang et al., 2019*). Moreover, although the rainwater NH_4^+ was not measured in the present study due to the inherent difficulty of the instrument (ICP-AES) for cations measurement, the previous rainwater nitrogen isotope-based studies have concluded that the rainwater NH_4^+ in Guiyang mainly from animal/human wastes (~22%), fertilizers (~22%), and agricultural biomass burning (~17%)(*Liu et al., 2017*; *Xiao et al., 2012*). This is highly in agreement with the characteristics (full of agricultural activities around the city and concentrated population in urban area) in such a developing city in southwest of China.

Deposition flux and potential environmental effects

Based on the ionic concentrations and the corresponding rainfall amount in each month during study period, the rainwater ions deposition fluxes are estimated (Fig. S4). There are fairly large ion deposition fluxes in such a karst city intensively impacted by human activities, with the range of 0.5 to 3.5 keq ha^{-1}, which is also a very high level over China (0.1–2.5 keq ha^{-1}) (*Rao et al., 2017*; *Yang et al., 2012*; *Zhao et al., 2008*; *Zhou et al., 2019*). As expected, the lowest monthly wet deposition flux is observed in July 2013 (Fig. S4) due to the extremely low rainfall amount in this month (26.4 mm) compared to the rainfall amount in other years (about 270–420 mm, Fig. S2B). These results suggest that both the sources contribution and the climatic conditions (e.g., rainfall amount) are responsible for the total ions wet deposition fluxes.

Moreover, the combination of protons in the aquatic ecosystems and nitrate and sulfate derived from wet deposition actuated water acidification in the hydrosphere have been a focus of environmental researches (*Chen et al., 2019*; *Qiao et al., 2018*), the wet deposition levels of sulfate and nitrate can therefore reflect the potential environmental effects of rainwater chemistry to some extent (*Pan et al., 2013*). This phenomenon significantly impacted the carbonate weathering in karst areas further influenced the global climate change (*Li et al., 2008*; *Liu & Han, 2020*; *Liu & Han, 2021*; *Raymond et al., 2013*; *Wang et al., 2019*). The previous studies on the aquatic ecosystem in Guiyang city also showed the enhanced carbonate rock weathering processes involved with exogenous sulfuric and nitric acid (*Lang et al., 2006*; *Zhong et al., 2018*). The monthly wet acid (nitrate and sulfate) deposition at Guiyang city ranged between 0.04 to 1.03 keq ha^{-1} (Fig. S5). The evaluated yearly wet acid deposition is 4.27 keq ha^{-1} $year^{-1}$ via the sum of each month's fluxes in 2013. This annual deposition flux is twice as much as in karst rural areas (*Zeng et al., 2020*). Different from the Yangtze River Delta (nitrate-dominated wet acid deposition) (*Chen et al., 2019*), the wet acid deposition in Guiyang city is controlled by the sulfur. The sulfur contributed significantly higher than the nitrate to total acid deposition with the mean monthly contribution rate of 88% (Fig. S5). Thus, the more detailed spatio-temporal monitoring of rainwater chemistry in karst urban area is necessary for understanding the rainfall-actuated acid deposition and its potential effects on hydrosphere, especially sulfate wet deposition (as an agent of weathering).

CONCLUSIONS

In conclusion, 26 monthly mixed rainwater samples collected in a karst city (Guiyang, 2012 to 2014) were investigated to explore the variations, influence factors and origins of ions. The rainwater ions composition varied obviously based on temporal rainwater chemistry investigation. Especially, Ca^{2+} and SO_4^{2-} concentrations range from 124.5 to 6,652.4 μeq L^{-1} and from 10.5 to 4,127.2 μeq L^{-1}, respectively. Ca^{2+}, Mg^{2+}, SO_4^{2-} and Cl^- are the most dominant ions with obviously monthly variations. Sources variations and precipitation amount are the vital affecting factors of rainwater ions, and the long-distance transportation is also non-negligible factor when precipitation amount exceed 100 mm. Source identification indicated that Mg^{2+}, Ca^{2+} and K^+ are predominantly influenced by the crustal sources (dust), while the anthropogenic emissions are the main origins of F^-, NO_3^- and SO_4^{2-}. Cl^- Enrichment in long-distance transport is the main contributor of Cl^-. The observed high level of total wet acid deposition implies the requirement of focus on rainfall-related acid deposition, particularly sulfur deposition as which is a potential weathering agent.

ACKNOWLEDGEMENTS

The authors thank Dr. Yang Tang from the Institute of Geochemistry, Chinese Academy of Sciences for sampling and laboratory work.

ADDITIONAL INFORMATION AND DECLARATIONS

Funding

This work was supported by the National Natural Science Foundation of China (Nos. 41325010 and 41661144029). The funders had no role in study design, data collection and analysis, decision to publish, or preparation of the manuscript.

Grant Disclosures

The following grant information was disclosed by the authors:
National Natural Science Foundation of China: 41325010 and 41661144029.

Competing Interests

The authors declare that they have no competing interests.

Author Contributions

- Jie Zeng analyzed the data, prepared figures and/or tables, authored or reviewed drafts of the paper, and approved the final draft.
- Guilin Han conceived and designed the experiments, performed the experiments, analyzed the data, prepared figures and/or tables, authored or reviewed drafts of the paper, and approved the final draft.

Data Availability

The following information was supplied regarding data availability:

Raw measurements are available in the Supplemental Files.

Supplemental Information

Supplemental information for this article can be found online at http://dx.doi.org/10.7717/peerj.11167#supplemental-information.

REFERENCES

Benedict KB, Prenni AJ, Sullivan AP, Evanoski-Cole AR, Fischer EV, Callahan S, Sive BC, Zhou Y, Schichtel BA, Collett JL. 2018. Impact of front range sources on reactive nitrogen concentrations and deposition in Rocky Mountain National Park. *PeerJ* **6(5)**:e4759 DOI 10.7717/peerj.4759.

Berner EK, Berner RA. 1987. *Global water cycle: geochemistry and environment*. New York: Prentice-Hall.

Bhattarai H, Zhang Y-L, Pavuluri CM, Wan X, Wu G, Li P, Cao F, Zhang W, Wang Y, Kang S, Ram K, Kawamura K, Ji Z, Widory D, Cong Z. 2019. Nitrogen speciation and isotopic composition of aerosols collected at Himalayan forest (3326 m a.s.l.): seasonality, sources, and implications. *Environmental Science & Technology* **53(21)**:12247–12256 DOI 10.1021/acs.est.9b03999.

Cable E, Deng Y. 2018. Trace elements in atmospheric wet precipitation in the detroit metropolitan area: levels and possible sources. *Chemosphere* **210**:1091–1098 DOI 10.1016/j.chemosphere.2018.07.103.

Cereceda-Balic F, De La Gala-Morales M, Palomo-Marín R, Fadic X, Vidal V, Funes M, Rueda-Holgado F, Pinilla-Gil E. 2020. Spatial distribution, sources, and risk assessment of major ions ad trace elements in rainwater at Puchuncaví Valley, Chile: the impact of industrial activities. *Atmospheric Pollution Research* **11(6)**:99–109 DOI 10.1016/j.apr.2020.03.003.

Chen Z, Huang T, Huang X, Han X, Yang H, Cai Z, Yao L, Han X, Zhang M, Huang C. 2019. Characteristics, sources and environmental implications of atmospheric wet nitrogen and sulfur deposition in Yangtze River Delta. *Atmospheric Environment* **219(18)**:116904 DOI 10.1016/j.atmosenv.2019.116904.

Cong Z, Kang S, Kawamura K, Liu B, Wan X, Wang Z, Gao S, Fu P, Kang S. 2015. Carbonaceous aerosols on the south edge of the Tibetan Plateau: concentrations, seasonality and sources. *Atmospheric Chemistry and Physics* **15(3)**:1573–1584 DOI 10.5194/acp-15-1573-2015.

Facchini Cerqueira MR, Pinto MF, Derossi IN, Esteves WT, Rachid Santos MD, Costa Matos MA, Lowinsohn D, Matos RC. 2014. Chemical characteristics of rainwater at a southeastern site of Brazil. *Atmospheric Pollution Research* **5(2)**:253–261 DOI 10.5094/APR.2014.031.

Garea A, Ortiz MI, Viguri JR, Renedo MJ, Fernandez J, Irabien JA. 1996. Desulfurization yield of calcium hydroxide/fly-ash mixtures. Thermogravimetric determination. *Thermochimica Acta* **286(1)**:173–185 DOI 10.1016/0040-6031(96)02930-9.

Gonçalves FLT, Ramos AM, Freitas S, Silva Dias MA, Massambani O. 2002. In-cloud and below-cloud numerical simulation of scavenging processes at Serra Do Mar region, SE Brazil. *Atmospheric Environment* **36(33)**:5245–5255 DOI 10.1016/S1352-2310(02)00461-2.

Han G, Liu C-Q. 2006. Strontium isotope and major ion chemistry of the rainwaters from Guiyang, Guizhou Province, China. *Science of the Total Environment* **364(1–3)**:165–174 DOI 10.1016/j.scitotenv.2005.06.025.

Han G, Song Z, Tang Y, Wu Q, Wang Z. 2019. Ca and Sr isotope compositions of rainwater from Guiyang city, Southwest China: implication for the sources of atmospheric aerosols and their

seasonal variations. *Atmospheric Environment* **214(5482)**:116854 DOI 10.1016/j.atmosenv.2019.116854.

Han G, Wu Q, Tang Y. 2011. Acid rain and alkalization in southwestern China: chemical and strontium isotope evidence in rainwater from Guiyang. *Journal of Atmospheric Chemistry* **68(2)**:139–155 DOI 10.1007/s10874-012-9213-x.

Jain CD, Madhavan BL, Ratnam MV. 2019. Source apportionment of rainwater chemical composition to investigate the transport of lower atmospheric pollutants to the UTLS region. *Environmental Pollution* **248**:166–174 DOI 10.1016/j.envpol.2019.02.007.

Jia G, Chen F. 2010. Monthly variations in nitrogen isotopes of ammonium and nitrate in wet deposition at Guangzhou, south China. *Atmospheric Environment* **44(19)**:2309–2315 DOI 10.1016/j.atmosenv.2010.03.041.

Jin Z, Wang Y, Qian L, Hu Y, Jin X, Hong C, Li F. 2019. Combining chemical components with stable isotopes to determine nitrate sources of precipitation in Hangzhou and Huzhou, SE China. *Atmospheric Pollution Research* **10(2)**:386–394 DOI 10.1016/j.apr.2018.09.004.

Keresztesi Á, Birsan M-V, Nita I-A, Bodor Z, Szép R. 2019. Assessing the neutralisation, wet deposition and source contributions of the precipitation chemistry over Europe during 2000–2017. *Environmental Sciences Europe* **31(1)**:50 DOI 10.1186/s12302-019-0234-9.

Keresztesi Á, Nita I-A, Birsan M-V, Bodor Z, Pernyeszi T, Micheu MM, Szép R. 2020a. Assessing the variations in the chemical composition of rainwater and air masses using the zonal and meridional index. *Atmospheric Research* **237**:104846 DOI 10.1016/j.atmosres.2020.104846.

Keresztesi Á, Nita I-A, Boga R, Birsan M-V, Bodor Z, Szép R. 2020b. Spatial and long-term analysis of rainwater chemistry over the conterminous United States. *Environmental Research* **188(50)**:109872 DOI 10.1016/j.envres.2020.109872.

Khare P, Goel A, Patel D, Behari J. 2004. Chemical characterization of rainwater at a developing urban habitat of Northern India. *Atmospheric Research* **69(3–4)**:135–145 DOI 10.1016/j.atmosres.2003.10.002.

Lang Y-C, Liu C-Q, Zhao Z-Q, Li S-L, Han G-L. 2006. Geochemistry of surface and ground water in Guiyang, China: water/rock interaction and pollution in a karst hydrological system. *Applied Geochemistry* **21(6)**:887–903 DOI 10.1016/j.apgeochem.2006.03.005.

Larssen T, Lydersen E, Tang D, He Y, Gao J, Liu H, Duan L, Seip HM, Vogt RD, Mulder J, Shao M, Wang Y, Shang H, Zhang X, Solberg S, Aas W, Okland T, Eilertsen O, Angell V, Li Q, Zhao D, Xiang R, Xiao J, Luo J. 2006. Acid rain in China. *Environmental Science & Technology* **40(2)**:418–425 DOI 10.1021/es0626133.

Li S-L, Calmels D, Han G, Gaillardet J, Liu C-Q. 2008. Sulfuric acid as an agent of carbonate weathering constrained by δ13CDIC: examples from Southwest China. *Earth and Planetary Science Letters* **270(3–4)**:189–199 DOI 10.1016/j.epsl.2008.02.039.

Li C, Li S-L, Yue F-J, He S-N, Shi Z-B, Di C-L, Liu C-Q. 2020a. Nitrate sources and formation of rainwater constrained by nitrate isotopes in Southeast Asia: example from Singapore. *Chemosphere* **241(D4)**:125024 DOI 10.1016/j.chemosphere.2019.125024.

Li M, Wang X, Lu C, Li R, Zhang J, Dong S, Yang L, Xue L, Chen J, Wang W. 2020b. Nitrated phenols and the phenolic precursors in the atmosphere in urban Jinan, China. *Science of the Total Environment* **714**:136760 DOI 10.1016/j.scitotenv.2020.136760.

Liu J, Han G. 2020. Major ions and δ34SSO4 in Jiulongjiang River water: investigating the relationships between natural chemical weathering and human perturbations. *Science of the Total Environment* **724(1)**:138208 DOI 10.1016/j.scitotenv.2020.138208.

Liu J, Han G. 2021. Tracing Riverine particulate black carbon sources in Xijiang river Basin: insight from stable isotopic composition and Bayesian mixing model. *Water Research* **194(3–4)**:116932 DOI 10.1016/j.watres.2021.116932.

Liu M, Han G, Zhang Q. 2020. Effects of agricultural abandonment on soil aggregation, soil organic carbon storage and stabilization: results from observation in a small karst catchment, Southwest China. *Agriculture, Ecosystems & Environment* **288**:106719 DOI 10.1016/j.agee.2019.106719.

Liu B, Kang S, Sun J, Zhang Y, Xu R, Wang Y, Liu Y, Cong Z. 2013. Wet precipitation chemistry at a high-altitude site (3,326 m a.s.l.) in the southeastern Tibetan Plateau. *Environmental Science and Pollution Research* **20(7)**:5013–5027 DOI 10.1007/s11356-012-1379-x.

Liu XY, Xiao HW, Xiao HY, Song W, Sun XC, Zheng XD, Liu CQ, Koba K. 2017. Stable isotope analyses of precipitation nitrogen sources in Guiyang, southwestern China. *Environmental Pollution* **230(4)**:486–494 DOI 10.1016/j.envpol.2017.06.010.

Lü P, Han G, Wu Q. 2017. Chemical characteristics of rainwater in karst rural areas, Guizhou Province, Southwest China. *Acta Geochimica* **36(3)**:572–576 DOI 10.1007/s11631-017-0238-3.

Martins EH, Nogarotto DC, Mortatti J, Pozza SA. 2019. Chemical composition of rainwater in an urban area of the southeast of Brazil. *Atmospheric Pollution Research* **10(2)**:520–530 DOI 10.1016/j.apr.2018.10.003.

Mullaugh KM, Hamilton JM, Avery GB, Felix JD, Mead RN, Willey JD, Kieber RJ. 2015. Temporal and spatial variability of trace volatile organic compounds in rainwater. *Chemosphere* **134**:203–209 DOI 10.1016/j.chemosphere.2015.04.027.

Naimabadi A, Shirmardi M, Maleki H, Teymouri P, Goudarzi G, Shahsavani A, Sorooshian A, Babaei AA, Mehrabi N, Baneshi MM, Zarei MR, Lababpour A, Ghozikali MG. 2018. On the chemical nature of precipitation in a populated Middle Eastern region (Ahvaz, Iran) with diverse sources. *Ecotoxicology and Environmental Safety* **163**:558–566 DOI 10.1016/j.ecoenv.2018.07.103.

Pan YP, Wang YS, Tang GQ, Wu D. 2013. Spatial distribution and temporal variations of atmospheric sulfur deposition in Northern China: insights into the potential acidification risks. *Atmospheric Chemistry and Physics* **13(3)**:1675–1688 DOI 10.5194/acp-13-1675-2013.

Qiao X, Du J, Kota SH, Ying Q, Xiao W, Tang Y. 2018. Wet deposition of sulfur and nitrogen in Jiuzhaigou National nature reserve, Sichuan, China during 2015–2016: possible effects from regional emission reduction and local tourist activities. *Environmental Pollution* **233(9)**:267–277 DOI 10.1016/j.envpol.2017.08.041.

Qin C, Li S-L, Waldron S, Yue F-J, Wang Z-J, Zhong J, Ding H, Liu C-Q. 2020. High-frequency monitoring reveals how hydrochemistry and dissolved carbon respond to rainstorms at a karstic critical zone, Southwestern China. *Science of the Total Environment* **714(1)**:136833 DOI 10.1016/j.scitotenv.2020.136833.

Rao W, Han G, Tan H, Jin K, Wang S, Chen T. 2017. Chemical and Sr isotopic characteristics of rainwater on the Alxa Desert Plateau, North China: implication for air quality and ion sources. *Atmospheric Research* **193**:163–172 DOI 10.1016/j.atmosres.2017.04.007.

Raymond PA, Hartmann J, Lauerwald R, Sobek S, McDonald C, Hoover M, Butman D, Striegl R, Mayorga E, Humborg C, Kortelainen P, Dürr H, Meybeck M, Ciais P, Guth P. 2013. Global carbon dioxide emissions from inland waters. *Nature* **503(7476)**:355–359 DOI 10.1038/nature12760.

Rouvalis A, Karadima C, Zioris IV, Sakkas VA, Albanis T, Iliopoulou-Georgudaki J. 2009. Determination of pesticides and toxic potency of rainwater samples in western Greece. *Ecotoxicology and Environmental Safety* **72(3)**:828–833 DOI 10.1016/j.ecoenv.2008.09.016.

Rudnick RL, Gao S. 2004. Composition of the continental crust. In: Rudnick RL, ed. *The Crust: Treatise on Geochemistry*. Oxford: Elsevier-Pergamon, 1–64.

Silva MPR, Gonçalves FLT, Freitas SR. 2009. Two case studies of sulfate scavenging processes in the Amazon region (Rondônia). *Environmental Pollution* **157(2)**:637–645 DOI 10.1016/j.envpol.2008.08.016.

Špičková J, Dobešová I, Vach M, Skřivan P, Mihaljevič M, Burian M. 2008. The influence of the limestone-quarry Čertovy schody (Czech Republic) on the precipitation chemistry and atmospheric deposition. *Chemie der Erde—Geochemistry* **68(1)**:105–115 DOI 10.1016/j.chemer.2005.11.004.

Szép R, Bodor Z, Miklóssy I, Niță I-A, Oprea OA, Keresztesi Á. 2019. Influence of peat fires on the rainwater chemistry in intra-mountain basins with specific atmospheric circulations (Eastern Carpathians, Romania). *Science of the Total Environment* **647**:275–289 DOI 10.1016/j.scitotenv.2018.07.462.

Szép R, Mateescu E, Niță I-A, Birsan M-V, Bodor Z, Keresztesi Á. 2018. Effects of the Eastern Carpathians on atmospheric circulations and precipitation chemistry from 2006 to 2016 at four monitoring stations (Eastern Carpathians, Romania). *Atmospheric Research* **214**:311–328 DOI 10.1016/j.atmosres.2018.08.009.

Vet R, Artz RS, Carou S, Shaw M, Ro C-U, Aas W, Baker A, Bowersox VC, Dentener F, Galy-Lacaux C, Hou A, Pienaar JJ, Gillett R, Forti MC, Gromov S, Hara H, Khodzher T, Mahowald NM, Nickovic S, Rao PSP, Reid NW. 2014. A global assessment of precipitation chemistry and deposition of sulfur, nitrogen, sea salt, base cations, organic acids, acidity and pH, and phosphorus. *Atmospheric Environment* **93(8)**:3–100 DOI 10.1016/j.atmosenv.2013.10.060.

Wang Z-J, Li S-L, Yue F-J, Qin C-Q, Buckerfield S, Zeng J. 2020. Rainfall driven nitrate transport in agricultural karst surface river system: insight from high resolution hydrochemistry and nitrate isotopes. *Agriculture, Ecosystems & Environment* **291**:106787 DOI 10.1016/j.agee.2019.106787.

Wang W-F, Li S-L, Zhong J, Maberly SC, Li C, Wang F-S, Xiao H-Y, Liu C-Q. 2019. Climatic and anthropogenic regulation of carbon transport and transformation in a karst river-reservoir system. *Science of the Total Environment* **707(7755)**:135628 DOI 10.1016/j.scitotenv.2019.135628.

Wang W, Sanku M, Karlsson H, Hulteberg C, Karlsson HT, Balfe M, Stallmann O. 2017a. Medium temperature desulfurization for oxyfuel and regenerative calcium cycle. *Energy Procedia* **114**:271–284 DOI 10.1016/j.egypro.2017.03.1169.

Wang ZJ, Yue FJ, Zeng J, Li SL. 2017b. The influence of urbanization on karst rivers based on nutrient concentration and nitrate dual isotopes: an example from southwestern China. *Acta Geochimica* **1–6(3)**:446–451 DOI 10.1007/s11631-017-0188-9.

Wei J, Huang W, Li Z, Xue W, Peng Y, Sun L, Cribb M. 2019. Estimating 1-km-resolution PM2.5 concentrations across China using the space-time random forest approach. *Remote Sensing of Environment* **231(10)**:111221 DOI 10.1016/j.rse.2019.111221.

Wei J, Li Z, Cribb M, Huang W, Xue W, Sun L, Guo J, Peng Y, Li J, Lyapustin A, Liu L, Wu H, Song Y. 2020. Improved 1 km resolution PM2.5 estimates across China using enhanced space-time extremely randomized trees. *Atmospheric Chemistry and Physics* **20(6)**:3273–3289 DOI 10.5194/acp-20-3273-2020.

Wen Z, Xu W, Li Q, Han M, Tang A, Zhang Y, Luo X, Shen J, Wang W, Li K, Pan Y, Zhang L, Li W, Collett JL, Zhong B, Wang X, Goulding K, Zhang F, Liu X. 2020. Changes of nitrogen deposition in China from 1980 to 2018. *Environment International* **144**:106022 DOI 10.1016/j.envint.2020.106022.

Wu Q, Han G, Tao F, Tang Y. 2012. Chemical composition of rainwater in a karstic agricultural area, Southwest China: the impact of urbanization. *Atmospheric Research* **111**:71–78 DOI 10.1016/j.atmosres.2012.03.002.

Xiao HY, Liu CQ. 2002. Sources of nitrogen and sulfur in wet deposition at Guiyang, southwest China. *Atmospheric Environment* **36(33)**:5121–5130 DOI 10.1016/S1352-2310(02)00649-0.

Xiao H-W, Xiao H-Y, Long A-M, Wang Y-L. 2012. Who controls the monthly variations of NH4+ nitrogen isotope composition in precipitation? *Atmospheric Environment* **54(6)**:201–206 DOI 10.1016/j.atmosenv.2012.02.035.

Xiao HW, Xiao HY, Long AM, Wang YL, Liu CQ. 2013. Chemical composition and source apportionment of rainwater at Guiyang, SW China. *Journal of Atmospheric Chemistry* **70(3)**:269–281 DOI 10.1007/s10874-013-9268-3.

Xiao H-W, Xiao H-Y, Zhang Z-Y, Wang Y-L, Long A-M, Liu CQ. 2016. Chemical characteristics and source apportionment of atmospheric precipitation in Yongxing Island. *China Environmental Science* **36**:3237–3244.

Xing J, Song J, Yuan H, Li X, Li N, Duan L, Qi D. 2019. Atmospheric wet deposition of dissolved organic carbon to a typical anthropogenic-influenced semi-enclosed bay in the western Yellow Sea, China: flux, sources and potential ecological environmental effects. *Ecotoxicology and Environmental Safety* **182**:109371 DOI 10.1016/j.ecoenv.2019.109371.

Xu S, Li S-L, Zhong J, Li C. 2020. Spatial scale effects of the variable relationships between landscape pattern and water quality: example from an agricultural karst river basin, Southwestern China. *Agriculture, Ecosystems & Environment* **300(4)**:106999 DOI 10.1016/j.agee.2020.106999.

Xu Z, Wu Y, Liu W-J, Liang C-S, Ji J, Zhao T, Zhang X. 2015. Chemical composition of rainwater and the acid neutralizing effect at Beijing and Chizhou city, China. *Atmospheric Research* **164–165(8)**:278–285 DOI 10.1016/j.atmosres.2015.05.009.

Yang J, Ge X, Wu Q. 2018. Temporal and spatial distribution characteristics of air quality index in Guiyang, China. *Resources and Environment in the Yangtze Basin* **27**:1827–1835 DOI 10.11870/cjlyzyyhj201808019.

Yang F, Tan J, Shi ZB, Cai Y, He K, Ma Y, Duan F, Okuda T, Tanaka S, Chen G. 2012. Five-year record of atmospheric precipitation chemistry in urban Beijing, China. *Atmospheric Chemistry and Physics* **12(4)**:2025–2035 DOI 10.5194/acp-12-2025-2012.

Yang X, Yu T, Zhang W, Qin J, Li H. 2019. Effect of rainwater-borne hydrogen peroxide on manure-derived Cu and Zn speciation distribution and bioavailability in rice-soil system. *Ecotoxicology and Environmental Safety* **177(11)**:1–6 DOI 10.1016/j.ecoenv.2019.03.108.

Yu G, Jia Y, He N, Zhu J, Chen Z, Wang Q, Piao S, Liu X, He H, Guo X, Wen Z, Li P, Ding G, Goulding K. 2019. Stabilization of atmospheric nitrogen deposition in China over the past decade. *Nature Geoscience* **12(6)**:424–429 DOI 10.1038/s41561-019-0352-4.

Yue F-J, Waldron S, Li S-L, Wang Z-J, Zeng J, Xu S, Zhang Z-C, Oliver DM. 2019. Land use interacts with changes in catchment hydrology to generate chronic nitrate pollution in karst waters and strong seasonality in excess nitrate export. *Science of the Total Environment* **696(16)**:134062 DOI 10.1016/j.scitotenv.2019.134062.

Zeng J, Han G. 2020. Preliminary copper isotope study on particulate matter in Zhujiang River, southwest China: application for source identification. *Ecotoxicology and Environmental Safety* **198**:110663 DOI 10.1016/j.ecoenv.2020.110663.

Zeng J, Yue F-J, Li S-L, Wang Z-J, Wu Q, Qin C-Q, Yan Z-L. 2020. Determining rainwater chemistry to reveal alkaline rain trend in Southwest China: evidence from a frequent-rainy karst

area with extensive agricultural production. *Environmental Pollution* **266(6)**:115166 DOI 10.1016/j.envpol.2020.115166.

Zhang C-H, Ma L-D. 2016. Ambient air quality trends in Guiyang during 2003–2014. *Journal of Environment and Health* **33**:432–434.

Zhang X, Xu Z, Liu W, Moon S, Zhao T, Zhou X, Zhang J, Wu Y, Jiang H, Zhou L. 2019. Hydrogeochemical and Sr isotope characteristics of the Yalong river Basin, Eastern Tibetan Plateau: implications for chemical weathering and controlling factors. *Geochemistry, Geophysics, Geosystems* **20(3)**:1221–1239 DOI 10.1029/2018GC007769.

Zhao Z, Tian L, Fischer E, Li Z, Jiao K. 2008. Study of chemical composition of precipitation at an alpine site and a rural site in the Urumqi River Valley, Eastern Tien Shan, China. *Atmospheric Environment* **42(39)**:8934–8942 DOI 10.1016/j.atmosenv.2008.08.003.

Zhong J, Li SL, Cai HM, Yue FJ, Tao FX. 2018. The response of carbon geochemistry to hydrological events within an Urban River, Southwestern China. *Geochemistry International* **56(5)**:462–473 DOI 10.1134/S0016702918050099.

Zhou X, Xu Z, Liu W, Wu Y, Zhao T, Jiang H, Zhang X, Zhang J, Zhou L, Wang Y. 2019. Chemical composition of precipitation in Shenzhen, a coastal mega-city in South China: influence of urbanization and anthropogenic activities on acidity and ionic composition. *Science of the Total Environment* **662(1)**:218–226 DOI 10.1016/j.scitotenv.2019.01.096.